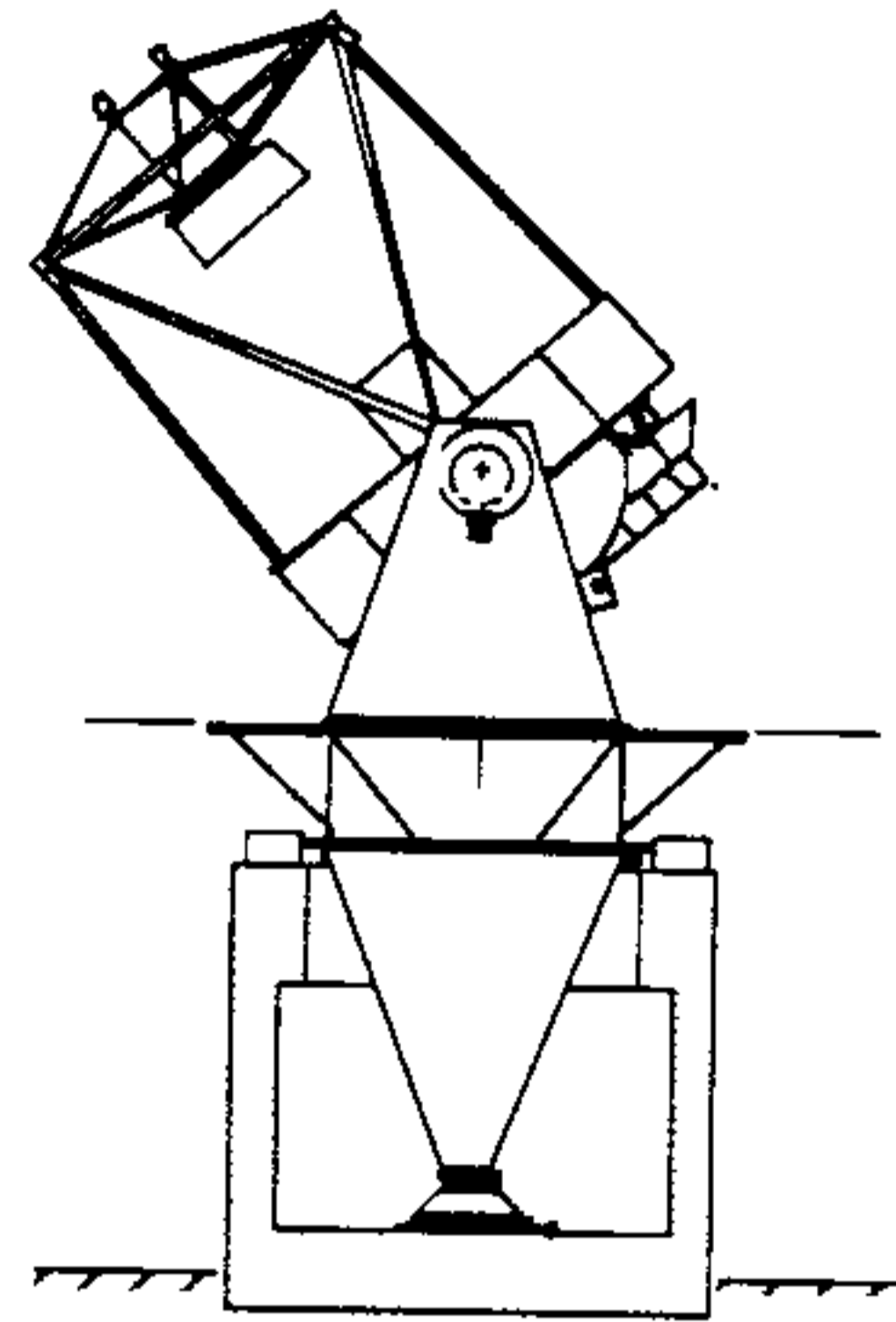


WISCONSIN  
INDIANA  
YALE  
NOAO



3.5 METER TELESCOPE

## 3.5 Meter Mirror Project at NOAO

L. Stepp

WODC 02-15-01

## 3.5m Mirror Project at NOAO

Larry Stepp

National Optical Astronomy Observatories<sup>††</sup>

P.O. Box 26732, Tucson, Arizona 85726-6732

ABSTRACT

At the National Optical Astronomy Observatories (NOAO) we have been working for several years to develop the technology for 8m telescopes using structured borosilicate glass primary mirrors. In March, 1989, we entered the final stage in this technology development program when we took delivery of a 3.5m mirror blank, cast under NOAO contract at the University of Arizona Mirror Lab. The NOAO 3.5m mirror project was established to develop and demonstrate technical innovations that will make possible successful 8m telescopes with borosilicate mirrors. The project will have four phases: 1) initial fabrication, 2) testing of support and thermal systems, 3) aspherizing the mirror and rework of the support and thermal systems, and 4) final acceptance test. At the conclusion of this effort we will have a finished 3.5m f/1.75 mirror, which will then become the heart of the new WIN telescope on Kitt Peak.

1. INTRODUCTION

NOAO has submitted a proposal to the National Science Foundation to build two 8m optical telescopes, one in the northern hemisphere and one in the southern. Construction of the 8m telescopes will present many technical challenges; some of the most interesting involve the primary mirror. The performance of the primary mirror is of paramount importance, and it is likely the primary mirror will be the most difficult component of the telescope to produce. Several factors will contribute to this difficulty: the size of the mirrors, the fast f/ratio proposed (f/1.8), the choice of mirror substrate (structured borosilicate glass), the excellent image quality required, and the need to control project cost.

Innovative engineering will be needed to solve problems in four areas: optical fabrication, optical testing, mirror supports and thermal control. The 3.5m mirror project provides an opportunity to develop technology at the 3.5m scale that will help ensure the success of the 8m telescopes.

2. TECHNICAL CHALLENGES: OPTICAL FABRICATION

The four areas of technical development mentioned above are interrelated, and optical fabrication is particularly dependent on the other three. Our ability to figure the mirror is directly limited by our optical testing capability. The mirror support must be designed to prevent distortion during polishing and testing. And with a borosilicate glass mirror, thermal control during optical fabrication is also important. While our concerns about optical testing, mirror support and thermal control do not end at the completion of optical fabrication, the accuracy of the polished surface is just as likely to be limited by these factors as by the skill of the optician.

The error budget for the polished figure of the 8m primary mirrors allows an image spread of 0.05 arc seconds. We would like to demonstrate this level of polishing accuracy in the work on the 3.5m mirror, even though the WIN telescope error budget allows 0.09 arc seconds for the polished figure.<sup>1</sup> The NOAO 8m Telescopes proposal contains a specification relating image size to wavefront error.<sup>2</sup> For low spatial frequencies the allowable RMS wavefront error  $\Delta Z$  is a function of the separation of measurement points  $d$ :

$$\Delta Z (d) = 130 d^{5/6} \quad (1)$$

<sup>††</sup>Operated by the Association of Universities for Research in Astronomy, Inc. under cooperative agreement with the National Science Foundation.

Z is measured in nanometers and d in meters. For high spatial frequencies wavefront errors must be less than 6nm RMS.

This specification can be related to particular types of polishing errors. High frequency ripple that might be caused by the use of small polishing tools must be limited to 6nm RMS. Print-through of the mirror's hexagonal structure would have a characteristic spacing (d) of about 20 cm and must be limited to 17 nm RMS. Print-through of the support locations would have a characteristic spacing of about 66 cm and must be limited to 46 nm RMS. Low spatial frequency errors, that might be caused by poor support during polishing or by thermal distortion during testing, must be limited to about 100 nm RMS.

To satisfy this specification we must meet a number of technical challenges. The mirror support used during polishing and testing must be repeatable, introduce minimal distortion, and match the telescope mirror support. Thermal distortion of the mirror blank during polishing and testing must be minimized. Polishing pressures must be kept low to minimize print-through of the hexagonal structure. The steeply curved f/1.8 hyperboloid must be polished accurately without introducing fine scale ripple and zonal defects. The mirror and its support systems must be able to withstand the polishing environment (mechanical forces, thermal conditions, chemical effects, etc.).

We believe large structured borosilicate mirrors, as fast as f/1.8, can be successfully polished to this level of accuracy in a reasonable amount of time, using extensions of traditional polishing techniques. We plan to demonstrate this in the 3.5m project. Other polishing techniques, for example the stressed lap method currently under development at the University of Arizona,<sup>3</sup> may be available by the time the 8m mirrors are polished; however we feel it is important to demonstrate that more traditional methods can be used if necessary.

### 3. TECHNICAL CHALLENGES: OPTICAL TESTING

One of the most important aspects of the 3.5m mirror project is optical testing, which will serve three important functions in the project. First, we will use optical tests to evaluate the performance of the mirror support, thermal control and active optics systems. These tests must provide accurate information about low spatial frequency departures from a spherical figure. Second, optical testing will guide the polishing work and provide the final acceptance test for the mirror. This will require the ability to test the highly aspheric mirror surface to an accuracy of a few nanometers, with spatial resolution of a few centimeters. Third, in the telescope optical test equipment will provide the feedback for our active optics system. We will need to measure the mirror's low spatial frequency figure errors -- using the light from a star -- without seriously affecting the use of the telescope for astronomy.

Each optical test has its limitations; to perform all of these functions more than one optical test method will be required. Moreover, the performance of any new test setup must be verified by comparison against other test methods, preferably ones that employ different physical principles. Therefore, we believe two independent test methods are required for each phase of optical testing.

For verification of mirror support, thermal control and active optics systems we plan to use subaperture Hartmann testing and interferometry. Both methods will use CCD cameras to record the images, and with our data reduction software we hope to show that both methods can provide results in a matter of minutes.

To guide fabrication of the aspheric mirror surface, we will use the wire test and a subaperture Hartmann test. Both of these can be performed on a highly aspheric surface without a null lens (the aspheric departure of the 3.5m mirror surface from a best fit sphere is 170 microns). In the final stages a scatterplate interferometer, equipped with a null lens, will be used to verify the results of the Hartmann test. The interferograms will be recorded on a CCD camera and analyzed using the Roddier method.<sup>4</sup> In addition to measuring low-frequency aberrations, this method will provide high spatial frequency information necessary to evaluate print-through and polishing ripple.<sup>5</sup> A method has been developed by Earl Pearson to obtain similar information from multiple subaperture Hartmann tests.<sup>5</sup> We expect both methods to provide spatial resolutions of a few centimeters. Comparisons between the two should also verify the performance of the null lens.

We plan to evaluate two optical testing approaches that could use the light from a star image to measure the mirror figure in the telescope. One is the Shack-Hartmann test, and the other is the curvature sensing technique.<sup>6</sup> Both of these will be evaluated in the optics shop, and their performance will be verified by comparison with the other test methods available. The more promising of the two methods will be incorporated into the design of the telescope.

#### 4. TECHNICAL CHALLENGES: MIRROR SUPPORTS

The 3.5m mirror support will follow the 8m mirror support design philosophy described in a previous paper.<sup>7</sup> The support will be designed to work adequately in a passive mode, but the axial support forces will have a variable component for active optics. Both the axial and lateral support forces will be applied at the back surface of the mirror blank. The resultant of the lateral support forces will not pass through the center of mass of the mirror, creating an overturning moment that must be compensated by forces from the axial supports.

Finite-element analysis has been used to design the support. The conclusions of this analysis will be described more fully in section 7.3, but several results are appropriate to this discussion of technical challenges. The WFN telescope error budget allows 0.09 arc seconds image spread for the mirror support. Our finite-element study indicated the error budget for axial support force errors should be 2.4 newtons each. The budget for lateral support force errors is 3.1 newtons each. The error budget for cross-talk errors such as transverse forces unintentionally applied by the axial support mechanisms is 2.7 newtons each. Our goal is to provide a support that meets these tolerances in its passive mode, at all zenith angles.

The accuracy of our finite-element analysis of structured mirrors is limited. The cast structure is more complex than the structural models we use, and there are small dimensional variations in the casting not reflected in the models. This does not invalidate the method, but it means the calculated support forces will likely be in error by more than the 2.4 newtons allowed. The precise forces needed to support the mirror with minimum distortion must be determined empirically. If the mirror support used during optical testing matches the support used in the telescope, distortions of the mirror caused by the axial supports can be polished out. These distortions will not be evident at the zenith, but their inverse will appear at the horizon along with any distortions produced by the lateral support. To determine the axial and lateral support forces that produce minimum mirror distortion at all zenith angles, testing at three different zenith angles is required. The NOAO large optics facility is set up to allow two testing orientations: zenith-pointing and horizon-pointing. Although testing in two orientations is significantly better than testing in only one orientation, it only allows the support to be optimized at two positions. Between the zenith and the horizon the support forces may still produce distortions that exceed our specifications.

Because of these possible force errors at intermediate zenith angles, and because there may be other distortions of the primary mirror caused by thermal gradients, polishing errors, etc., we believe active optics will be needed. We hope to demonstrate successful active optics capabilities in the 3.5m mirror support. One of the most challenging tasks will be to develop a system that changes the support forces without producing image shifts.

The support system must also protect the mirror, for example it should prevent damage to the mirror in case of an earthquake. And finally, the support system must be designed to work reliably for years without extensive maintenance.

#### 5. TECHNICAL CHALLENGES: THERMAL CONTROL

Control of primary mirror temperature is now recognized as an important factor in the design of large telescopes. If the difference between the temperature of the mirror and the temperature of the air above it is greater than about 0.6 °C, mirror seeing can degrade the image.<sup>8</sup> Structured borosilicate mirrors are also susceptible to distortions caused by temperature variations in the glass. Finite-element analysis indicates image degradation of about 0.5 arc seconds per degree can be expected for a structured borosilicate mirror with an aspect ratio of 9:1.<sup>9</sup>

We plan to control the 3.5m mirror temperature with an active ventilation system. NOAO is currently collaborating with Apache Point Observatory (APO) and the Magellan Project in a thermal control experiment, making use of the APO 3.5m telescope structure and enclosure.<sup>10</sup> In this experiment the most successful thermal control system has been a variation on designs developed at the University of Arizona.<sup>11,12</sup> The thermal control system for our 3.5m mirror will be similar.

To evaluate the performance of the thermal control system we need to know the temperature at several hundred different points in the glass, and additional sensors will be needed to monitor the operation of the thermal control system itself. These sensors must be quite accurate. The WFN telescope error budget for thermal uniformity of the primary mirror is  $\pm 0.12^\circ\text{C}$ , or about  $\pm 0.03^\circ\text{RMS}$ . Therefore, the thermal sensors should be able to make relative temperature measurements with an accuracy of better than  $0.01^\circ\text{C RMS}$ .

During our tests the thermal environment around the mirror should simulate the expected environment in the telescope. To accomplish this we will need to test the mirror and thermal control system mounted in the actual telescope mirror cell. The optical surface must be aluminized to prevent heat transfer to the front surface by radiation. The test facility will need a means for creating air flows and temperature changes in the environment around the mirror cell. While running thermal tests we will need to perform simultaneous optical tests to measure the distortion of the mirror surface.

## 6. PLAN FOR THE PROJECT

The plan for our 3.5m mirror project is a little unusual. Usually, when fabricating an aspheric mirror for a telescope, the mirror is polished to a spherical figure and then almost immediately aspherizing is begun. We plan to leave this mirror spherical for most of a year. We also plan to aluminize the mirror while it is spherical. Most telescope projects design and build the mirror supports once. We will design and build our mirror supports twice. The same is true for our thermal control system. We are building the mirror cell early in the project, two years before it is needed for installation in the telescope. And although most telescope mirrors made in the past were tested only in one orientation, usually either zenith-pointing or horizon-pointing, we plan to test the 3.5m mirror in both of these orientations.

### 6.1 Phase I

The project is divided into four phases; at present we are still in phase I. In this phase the mirror blank has been generated to its approximate finished dimensions and the optical surface has been ground to a radius of curvature of 12.32 meters. Currently the optical surface is being polished to a spherical figure to facilitate optical testing from the center of curvature. After completion of polishing the mirror will be aluminized in the 4-meter coating chamber on Kitt Peak.

During phase I the mirror cell, support system, thermal control system, and temperature monitoring system are being designed and built, although we expect to make improvements to their designs in phase III. We are also preparing optical test equipment and writing optical and thermal data reduction software.

### 6.2 Phase II

The second phase is primarily a testing phase. During this phase the mirror, supports and thermal control system will be assembled in the mirror cell, along with a system of thermal sensors. This assembly will be mounted on the polishing machine table, which can be tilted to allow optical testing of the mirror in zenith-pointing and horizon-pointing orientations. We will measure the positional shift of the mirror relative to the mirror cell as we change the zenith angle, and we will develop a system that will allow us to adjust the position and tilt of the mirror to maintain alignment in the telescope.

The performance of the mirror supports in passive mode will be evaluated by optical tests performed at the zenith and horizon. Presumably the mirror figure will look good at zenith-pointing, because the mirror will have been figured on the basis of optical tests performed on a support that matches the support in the mirror cell. However, we anticipate the figure will not look as good at the horizon. Corrections will be made to the horizon-pointing figure using the active optics part of the support system. These corrections will then be incorporated into the redesign of the supports in phase III. Note that with tests at only two orientations, we will have to guess which part of the distortion we see at the horizon comes from incorrectly calculated axial support forces, and which part comes from incorrect forces in the lateral support.

The capabilities of the active optics system will be explored in a series of tests. We will introduce errors, for example with an uneven thermal input, and then evaluate the ability of the active optics system to correct the errors. Another test will involve the intentional production of specific aberration terms such as astigmatism, or coma. This capability will provide a distinct advantage for our optical test development work. We will be able to develop optical test methods, and compare one test method to another, in a facility that offers programmable aberrations.

The performance of the thermal control system will also be evaluated, and adjustments will be made to refine its performance. We believe the inertia of the polishing machine table is comparable to the inertia of the telescope optical support structure, so we will be able to characterize any vibration problems caused by the thermal control system by making accelerometer measurements and performing optical tests while the blowers are running.

While this testing is in progress our opticians will be fabricating the null lens and experimenting with aspheric polishing methods using semi-flexible laps. At the end of phase II the mirror cell assembly will be removed from the polishing machine table, the mirror will be removed from the cell, and the polishing setup (adjusted to provide the newly defined support forces) will be reconstructed on the table.

### 6.3 Phase III

In phase III the mirror will be polished to the modified hyperbolic figure required by its Ritchey-Chretien design. Further experimentation in aspheric polishing methods will probably be required during this effort. When the mirror has been figured to the required accuracy, it will be aluminized again. While polishing is underway the mirror cell, support system and thermal control system will be redesigned and rebuilt to incorporate the empirically-derived set of support forces, and to solve any performance problems that were identified during phase II. At this time the computerized controls for the active optics, active alignment, and thermal control systems will be integrated into the telescope control systems.

### 6.4 Phase IV

The fourth phase in the project will be the final acceptance test. The aluminized mirror will be installed in the mirror cell with all support and thermal control systems in place, but with only a few thermal sensors remaining. A final series of optical tests will confirm the performance of the mirror in zenith-pointing and horizon-pointing orientations. Last minute adjustments will be made, then the mirror and cell will be shipped to Kitt Peak for incorporation into the WFN telescope.

## 7. PROGRESS TO DATE

### 7.1 Optical fabrication

When the mirror blank first arrived at our facility we placed it on the polishing table face down on an adjustable 3-point support (see Figure 1) and then spent several days measuring its geometry. We constructed a long-armed dial caliper (shown in Figure 2) and used it to measure the thickness of the 804 individual rib segments at four different heights. We also measured the thickness of the outer wall at four heights for 60 different azimuth positions, and the thickness of the inner wall at three heights for 18 different azimuth positions. These measurements are summarized in Table 1.

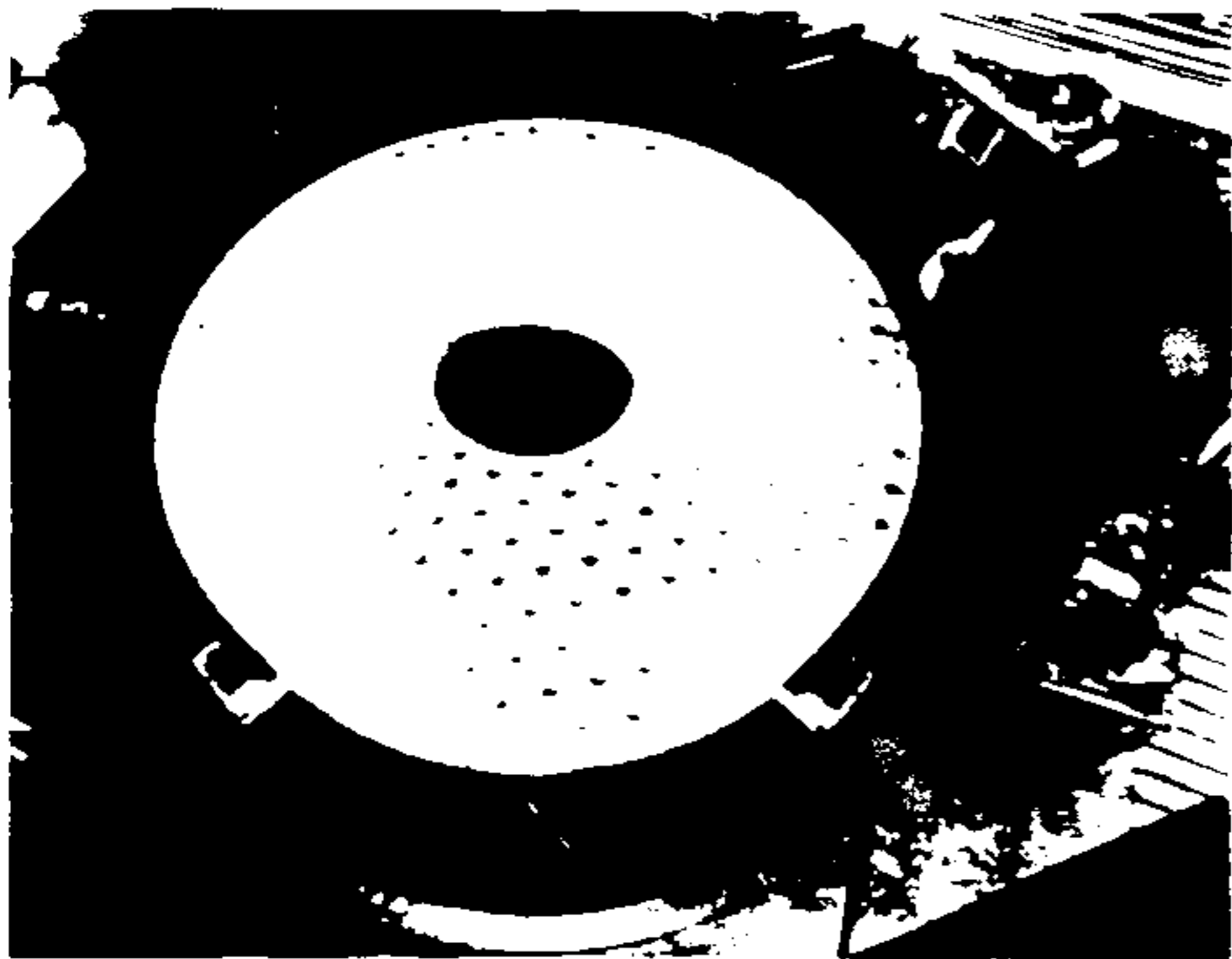


Figure 1. The 3.5m mirror blank has been placed face down on a three-point support for generating the back surface.

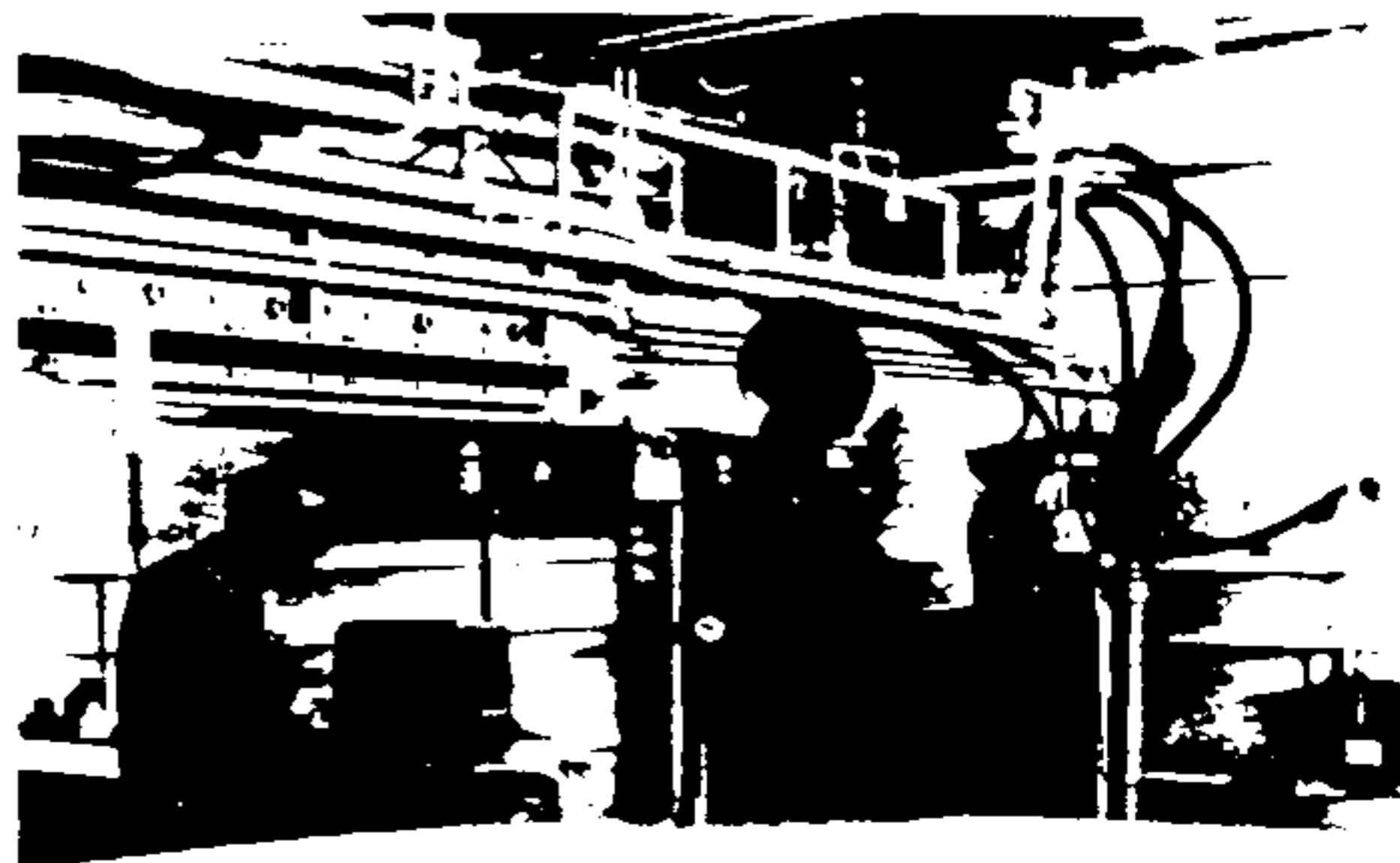


Figure 2. A specially-constructed dial caliper is used to measure the thickness of the ribs in the mirror at different depths.

Table 1  
Summary of measurements of rib thickness.

	Minimum (mm)	Maximum (mm)	Average (mm)	Std. Dev. (mm)
<b>Rib Thickness</b>				
75 mm from back surface	9.96	13.72	11.53	0.55
200 mm from back surface	10.26	13.03	11.28	0.42
275 mm from back surface	10.41	13.00	11.18	0.40
375 mm from back surface	9.91	13.16	11.33	0.54
<b>Outer Wall Thickness</b>				
75 mm from back surface	12.62	18.03	15.27	1.18
200 mm from back surface	12.98	18.41	15.39	1.24
275 mm from back surface	12.22	17.50	15.00	1.29
375 mm from back surface	10.87	16.41	13.89	1.41
<b>Inner Wall Thickness</b>				
75 mm from back surface	11.68	14.38	12.64	0.75
200 mm from back surface	12.42	15.75	13.63	0.97
275 mm from back surface	11.86	16.48	13.53	1.28

The thickness of the back faceplate was measured at each hexagonal cell around the outer and inner edges of the mirror, using a micrometer caliper. Because of the roughness of the cast surface the thickness was measured at three locations in each hexagon and the three measurements were averaged. An acoustic thickness gage was used to measure the thickness of the front faceplate in the cells around the outer and inner edges. Months later, after we completed generating and grinding, the thickness of the front and back faceplates was measured at each of the 294 hexagonal cells. These measurements are summarized in Table 2.

Table 2  
Summary of measurements of front and back faceplate thicknesses.

	Minimum (mm)	Maximum (mm)	Average (mm)	Std. Dev. (mm)
<b>Back Plate Thickness</b>				
As-cast: outer cells	31.11	33.91	32.61	0.67
As-cast: inner cells	31.95	34.62	33.16	0.80
Finished Dimensions: all cells	24.88	28.37	26.27	0.46
<b>Front Plate Thickness</b>				
As-cast: outer cells	42.17	44.64	43.47	0.57
As-cast: inner cells	39.84	43.87	42.13	0.98
Finished Dimensions: all cells	27.18	31.95	30.14	0.60

Our initial measurements indicated the front and back faceplates had a small amount of wedge (approximately 0.75 mm each) with similar orientation. Therefore we tilted the mirror blank slightly before we started generating, and some of this thickness variation was removed during generating. The mirror blank was centered by rotating the table and measuring the runout using a dial indicator with a roller tip, running on the side wall of the mirror approximately halfway between front and back. The side wall was slightly out of round, with a total runout (once the mirror was centered) of 1.5 mm in the radial direction. It also was slightly barrel shaped, bulging approximately 1 mm compared to a true cylinder.

To generate the mirror blank we used a 300 mm diamond wheel mounted on a grinding spindle attached to the 4-meter polishing machine. To prevent coolant from filling up the hollow mirror structure we made 294 rubber stoppers by cutting

disks out of 12 mm thick rubber sheet. These were pressed into the holes in the back of the mirror. We generated the outside and inside diameters of the back rim, and put generous bevels on the edges. Then we generated the back of the mirror flat, removing approximately 5 mm of glass from the back surface (see Figure 3). Most of the material was removed with a 60-grit wheel, but a 220-grit wheel was used for the finish cuts. The rib wall around the central hole of the mirror blank was also smoothed by generating.

After generating, the holes in the back of the blank had sharp edges. We constructed a compressed air driven beveling grinder and beveled the edge of each hole with a diamond grinding wheel. To smooth the bevels further and remove subsurface damage, the bevels were finished by hand-grinding with a hemispherical cast iron tool and loose abrasives. These tools are shown in Figure 4.



Figure 3. Generating the flat back of the mirror with a diamond wheel. The holes in the back of the mirror have been plugged with rubber disks.



Figure 4. Tools used to bevel the sharp edges of the holes in the back of the mirror blank.

The back surface was flattened further by grinding with a 1.4-meter diameter flat tool and loose abrasives -- first 80 grit, then 220 grit. At the same time we ground the side wall of the mirror blank smooth using a flexible perforated stainless steel band extending around one fourth of the circumference (see Figure 5). As the abrasive was washed over the outer edge of the mirror by the grinding action it ran between the perforated band and the side of the mirror, thereby grinding two surfaces with one charge of abrasive. After grinding, measurements indicated the back was flat to about 60 microns.

After we completed grinding the back of the blank it was etched with hydrofluoric acid. This was done to strengthen the blank by rounding out microscopic subsurface cracks. The rubber stoppers were pushed down to expose as much of the inside edges of the holes as possible -- about 12 mm. A rubber strip was clamped to the outside edge of the mirror blank with steel banding strap, and another was clamped to the inside edge with a rigid steel ring (see Figure 6). Taking extensive precautions to protect personnel and equipment, we flooded the back surface of the mirror with a lake of acid about 20 mm thick. Additional acid was wiped on the outside wall of the blank. Ground glass witness samples had been placed on several of the rubber stoppers; these were removed periodically and examined with a microscope. After one hour the microscopic cracks were visibly rounded out. The acid was then neutralized in place by the addition of large quantities of diluted sodium hydroxide.

After etching was completed the level of stress in the casting was evaluated by Blain Olbert of the Steward Observatory Mirror Lab (SOML). He used a Soleil-Babinet compensator to measure the strain-induced birefringence (Figure 7). His strain measurements (averaged over the thickness of the blank) indicated a maximum stress level of 87 psi. At most locations in the blank the average stress was about half of this level.





Figure 5. Loose abrasive grinding the back of the mirror with a flat tool, and the side of the mirror with a flexible perforated band.



Figure 6. The back of the mirror was etched with hydrofluoric acid to alleviate subsurface damage.

The blank was turned over and the curved front surface was generated. The cut was started at the inside diameter and spiraled outwards as the mirror blank rotated (see Figure 8). Our polishing machine is not computer controlled, but we recently mounted encoders on each of its axes of motion. The optician monitored the progress of the grinding wheel on a computer terminal, comparing its position to the programmed position. Approximately once every 10 seconds the grinder was jogged upwards about 10 microns, following the programmed curve. The rate of glass removal was kept constant at about 30 cubic centimeters per minute by gradually reducing the radial velocity as the cut progressed. The depth of each cut was about 3 mm -- four 12-hour cuts were required to remove 11 mm of glass from the front surface.



Figure 7. Evaluating internal stresses by measuring strain-induced birefringence.

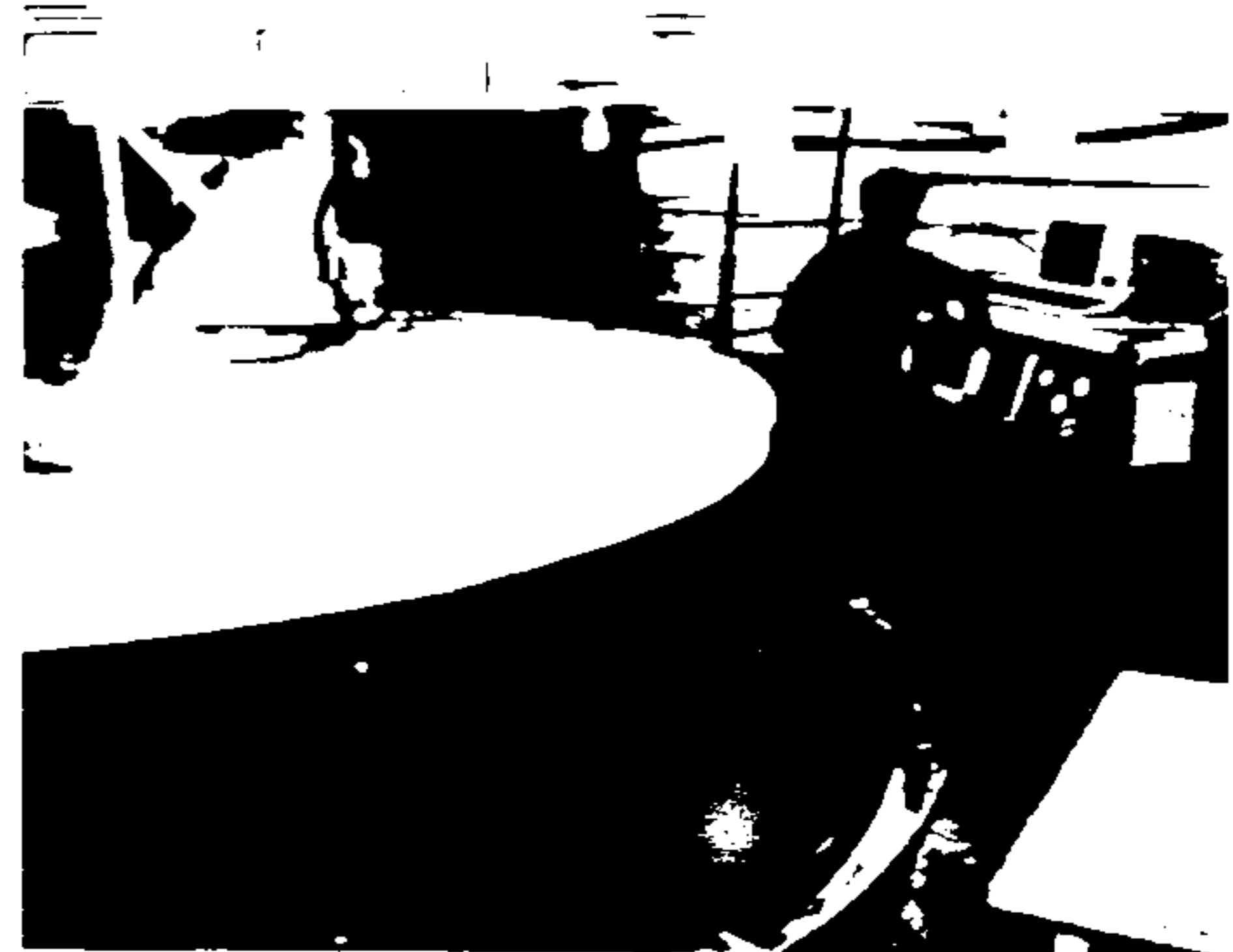


Figure 8. Generating the front surface by manually adjusting the grinder height to follow the programmed curve.

The mirror blank is remarkably bubble-free. After generating there was only one bubble of any significant size breaking the optical surface. It was about 1 cm in diameter. The bubble was ground out to form a smooth-walled tapered hole. A

machined plug of E-6 glass from the same melt was carefully lapped in with loose abrasive and then bonded in place with epoxy. Figure 9 shows the plug and hole before gluing, and again after gluing and then grinding with 80 grit.



Figure 9. The E-6 glass plug and the ground out bubble before gluing (left) and after gluing and 80 grit grinding (right).

After the completion of generating the mirror was removed from the polishing machine table. Several weeks were spent installing the polishing/testing support on the table. At the same time thermal sensors were installed in the mirror blank.

The mirror was then replaced on the polishing machine and we started loose abrasive grinding. Grinding with 80 grit silicon carbide smoothed the surface and removed the subsurface damage left by generating. About 1.6 mm of material was removed with 80 grit. Grinding continued with 220 grit silicon carbide, then 25 micron and 9 micron aluminum oxide. These three finer grits removed approximately 0.7 mm more glass. We have now started polishing with 3 micron cerium oxide; the final figuring will be done with rouge.

### 7.2 Optical testing

One of our optical test methods for large optics uses a scatterplate interferometer. Interferograms with 60 to 80 fringes of tilt across the aperture are recorded by a 512 x 512 pixel CCD camera. Fourier transform techniques are used to produce a phase map of the surface. This method is described in a paper recently submitted to *Optical Engineering*.<sup>13</sup> During the past year we have upgraded our equipment to handle the  $f/3.5$  beam required to test this mirror at its center of curvature, and we have built platforms in our test tower at the correct height above the polishing machine.

Another optical test method used extensively at NOAO in the past is the Hartmann test. The modified form of Hartmann test recently developed by Earl Pearson uses a screen that covers one quarter of the mirror. It can be placed over each quadrant of the mirror sequentially to provide full coverage of the optical surface, and it can also be moved in a raster pattern by increments of half the hole spacing in each direction to provide better spatial resolution. The spot images will be recorded by a Photometrics 1024 x 1000 CCD camera. This camera has been received, the data reduction software has been written, and we are currently fabricating the camera mounting assembly, the screen and its kinematic supports.

We are also working on the design of Shack-Hartmann test equipment. We have recently received a batch of lenslet arrays fabricated for us by Corning. These are 24 x 24 arrays of 1/2 mm diameter lenslets, with a focal length of 35 mm.

### 7.3 Mirror support

To develop the support design, we started by studying several possible patterns of axial support locations. We chose to locate the supports at rib junctions on the back of the mirror; several likely looking support patterns were selected, ranging from as many as 90 supports to as few as 66 supports. Finite-element analysis of load cases with unit loads applied at each

support gave us displacement information that we combined into an influence coefficient matrix. The magnitudes of the support forces were optimized by a least-squares fit that minimized the distortion of the optical surface. Five different support patterns were optimized in this manner. The pattern with the minimum number of supports (66) was judged to provide acceptable performance (a distortion resulting in 0.08 arc seconds FWHM of image spread) so it was selected. This pattern is shown in Figure 10. The optimized forces for this axial support range from 211 to 425 newtons.

The position of the mirror will be defined by the axial supports rather than by three hard points; any external disturbing force such as the wind will be resisted by all 66 supports. The support system as a whole must be stiff to maintain alignment in the telescope, however, we want each individual support mechanism to be astatic -- exerting the correct force regardless of its relative position. The spring constant of the system should be high, while the spring constant of each individual support should be as low as possible. To accomplish this, the axial support system has been designed as a hydraulic whiffle-tree. Each support will incorporate a liquid-filled diaphragm cylinder; these will be connected together in three groups of 22, forming a statically determinant system. Active alignment may be required in the telescope; we plan to tilt the primary mirror if necessary by adjusting the fluid level in each zone of supports under computer control.

For simplicity we want to use catalog sizes of diaphragm cylinders if possible. We chose a series of diaphragm sizes from the Bellofram catalog and fit the required forces to the areas of these diaphragms in much the same way lens radii in an optical design are fit to test plates. After eleven reoptimizations with increasing numbers of constraints we had fitted all the forces to catalog sizes. These modified forces were applied to the finite-element model and the resulting optical surface distortions were still quite acceptable. The testing supports and the first generation telescope supports have been designed using these cylinder sizes, however we expect to make minor changes after two-position testing.

The lateral supports will apply transverse forces to the mirror in the plane of the back plate, through levers bearing on the sides of the holes in the back of the mirror. We used a series of least squares fits to guide us in choosing the particular holes at which to apply the lateral forces. Forty potential positions, distributed over the back of the mirror, were studied. Individual unit force load cases were analyzed for each position. Displacement information from the 66 axial and 40 lateral unit load cases was combined into an influence coefficient matrix, and a least-squares fit determined the optimum forces for horizon-pointing support. Some of the lateral forces determined by the least-squares fit were negative, in other words, the support forces would be downward. The supports at these locations were eliminated. The optimization was repeated with fewer lateral locations included, and this time any lateral supports with negative or small forces were eliminated. After several iterations of this type the number of lateral supports was reduced to 24. It could have been reduced further (the distortions were acceptable with as few as 18 lateral supports) but we chose to retain 24 lateral supports to prevent the force applied at each support from getting too large. The chosen positions are shown in Figure 11.

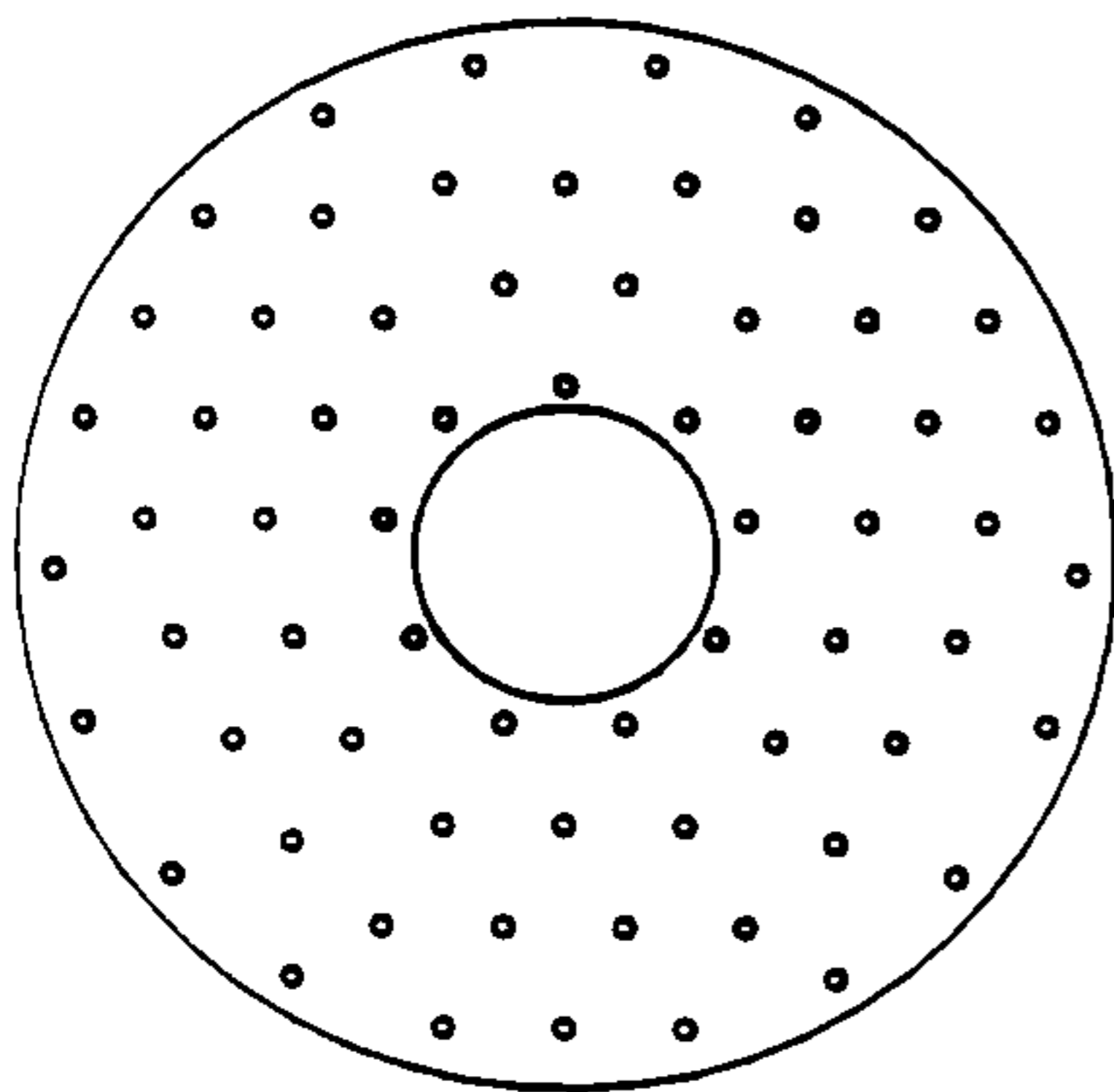


Figure 10. Locations of the 66 axial supports.

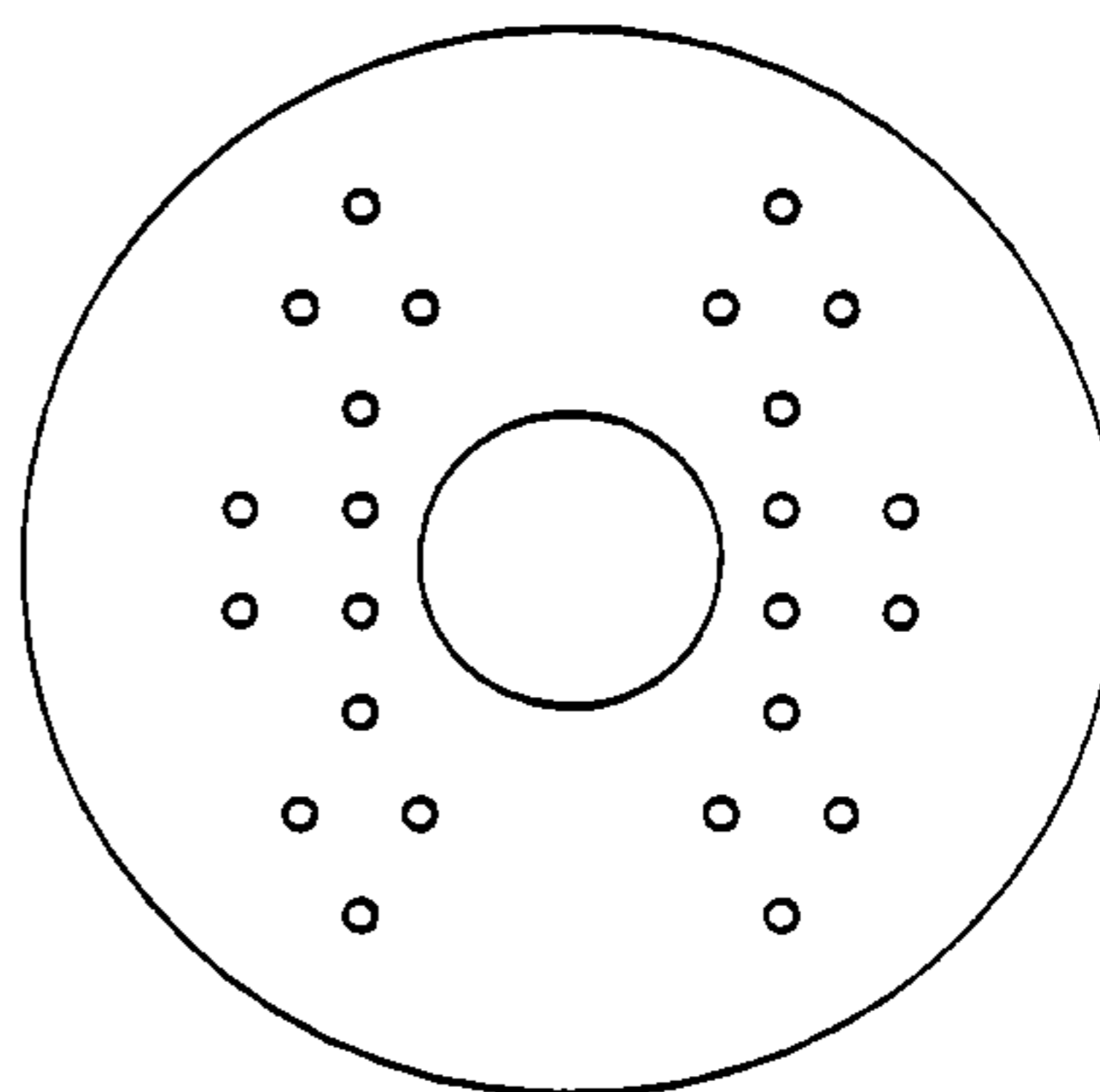


Figure 11. Locations of the 24 lateral supports.

The lateral support mechanisms are compound levers that transfer the weight of the mirror to a closed system of liquid-filled diaphragm cylinders. All of the cylinders are linked together in a closed system; each individual mechanism is astatic but the entire system resists downward lateral motion. For ease of fabrication we decided to make all the lateral support mechanisms identical. The only variation in force between individual supports is caused by hydrostatic pressure variations in the system. After the force at each lateral support was determined, the horizon-pointing least-squares fit optimization was redone to determine the forces required at the axial supports. The optical surface resulting from these modified forces was still quite acceptable.

Three years ago we performed active optics experiments using a 1.8m borosilicate mirror.<sup>14</sup> The active optics system for the 3.5m mirror will work on the same principles, except instead of modal precalculation of the figure changes we plan to perform real time least-squares fits to minimize the optical surface distortion at a large number of points on a square grid. We have already performed the finite-element analysis necessary to set up the active optics calculations. To evaluate the potential for correcting mirror distortions we calculated the forces needed to produce 33 different mirror figures, corresponding to 33 terms in the Zernike polynomial. Our calculations show that with this mirror and set of support locations we should be able to produce 16 of the lower order Zernike terms with reasonable accuracy using moderate forces.

During polishing the mirror must be supported with a minimum of distortion, but each support should also be relatively stiff to resist local deformations caused by the shifting forces applied by the polishing tool. For testing the mirror should be floated on a support that matches the support used in the telescope. It is also convenient if the mirror can be tilted through small angles to aid alignment with the test equipment. We have designed a dual polishing/testing support to meet these needs (see Figure 12). The testing support is three zones of 22 diaphragm cylinders, matching the passive portion of the telescope mirror support. By adjusting the fluid level in each zone the mirror can be tilted for alignment. Around each testing support piston is a ring of rubber; when the hydraulic pressure is released the mirror settles down onto these 66 rubber rings. The area of each ring is in proportion to the area in its associated cylinder, so if the deflections of the rubber rings under load can be kept equal, the forces applied by the polishing support will approximately match those applied by the testing support. We went to considerable effort to ensure the deflections will be nearly equal by grinding the back of the mirror flat, grinding the rubber rings to identical thickness, and machining the tops of the cylinder housings in place on the polishing table.

#### 7.4 Thermal control

The thermal sensor we chose for the 3.5m mirror thermal monitoring system is the AD592 sensor made by Analog Devices, Inc. The output of these devices is a current linearly proportional to the temperature. A system of 1024 of these sensors has been assembled and calibrated, and over the temperature range of our experiments (-5 C to + 30 C) the accuracy of these sensors appears to be about 0.005° C RMS.<sup>15</sup>

To avoid bonding the thermal sensors directly to the inside surfaces of the mirror structure, we made spring loaded mounting rods to hold the sensors against the glass. These are shown in Figure 13. The springs are quite soft; their effect on the mirror figure has been checked by finite-element analysis and it is negligible. Each rod holds three sensors: one is held against the front faceplate of the mirror, one is held against the back faceplate, and one measures the air temperature in the center of the cell. Each of the 294 hexagonal cells in the mirror contains one of these assemblies, placed diagonally across the cell from front to back. In addition, 60 sensors are bonded to the glass at locations around the outer diameter, and 18 are bonded to the mirror around the inner diameter. All of these sensors are now in place in the mirror. Another 64 sensors are available for monitoring other parts of the thermal control system and environment.

The mirror cell is designed to incorporate the ventilation system we will use for thermal control. The cell will be a welded steel sandwich structure. The central space will be used as an air plenum to supply air to 354 nozzles that ventilate the mirror. Return air will flow behind the back of the mirror to its inner and outer edges. There blowers will force the air through heat exchangers to condition the air before returning it to the plenum space. A chiller located some distance away from the telescope will supply controlled-temperature liquid to the heat exchangers.

A full scale plywood mockup of 1/12 of the mirror cell has been constructed and will be used in experiments designed to characterize the air flow patterns in the mirror cell. Flow-directing vanes will be installed if needed.

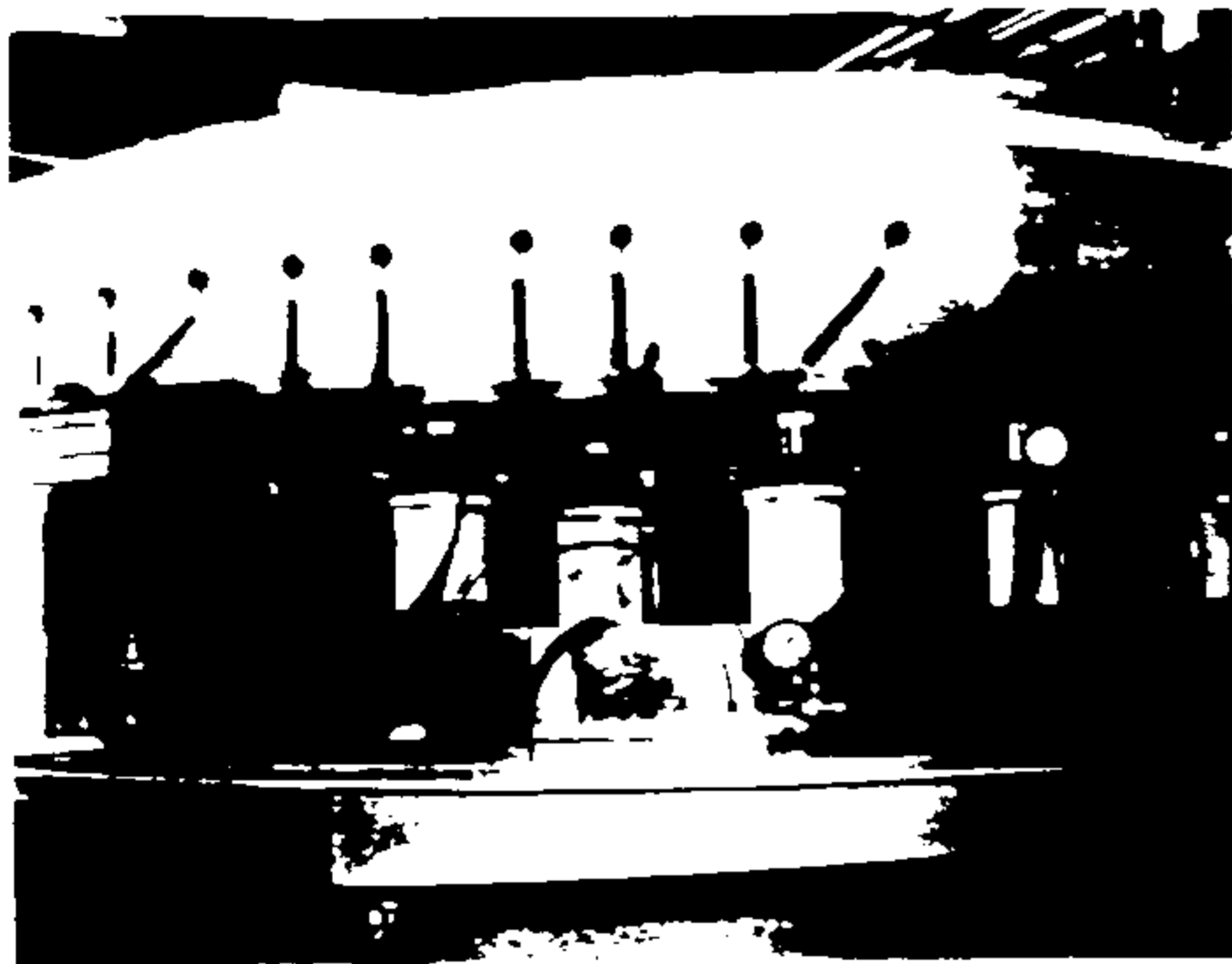


Figure 12. View of the polishing/testing supports. The ribbon cables connect thermal sensors to the junction box at left.

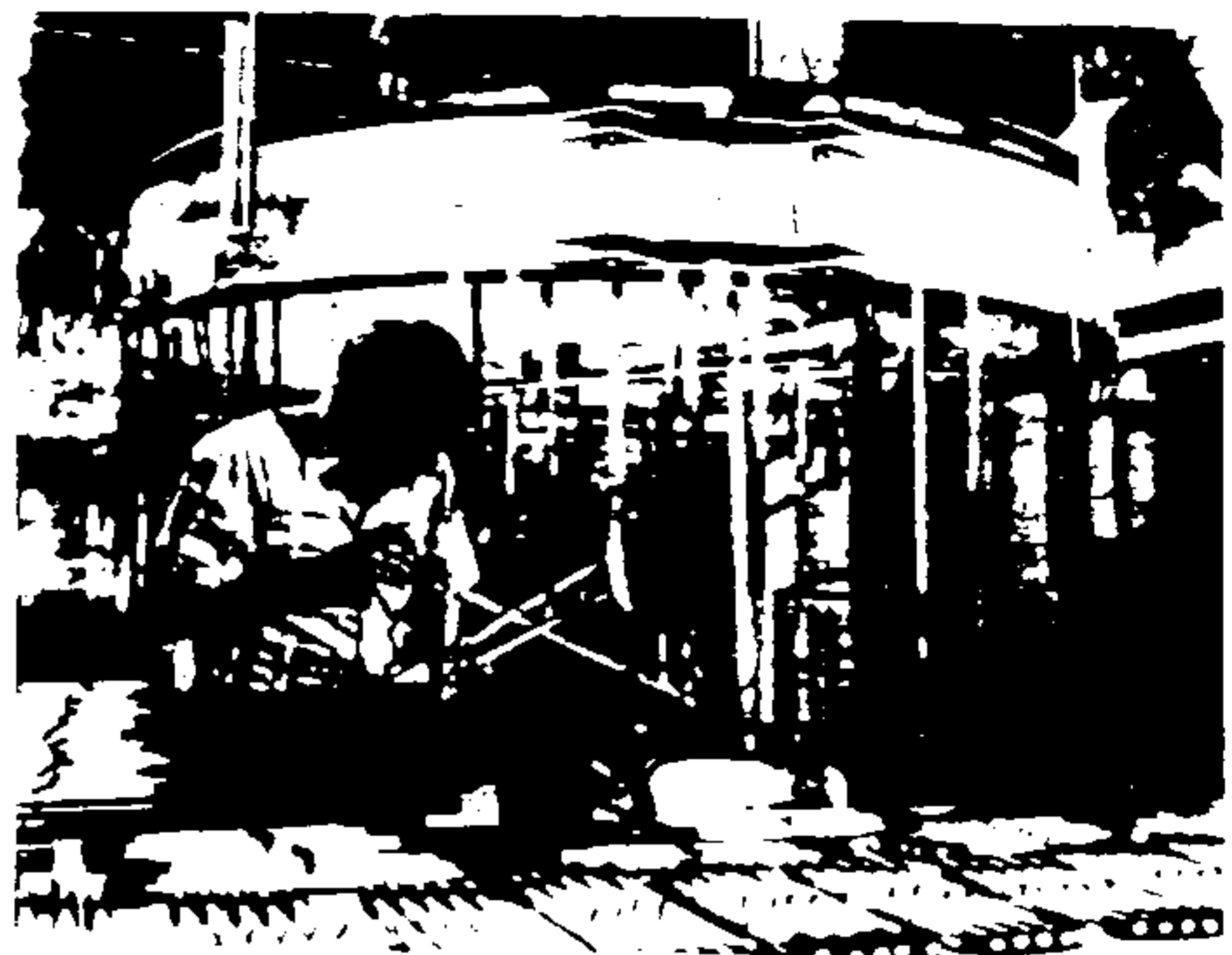


Figure 13. Some of the 294 thermal sensor assemblies ready for installation in the mirror.

### 8. CONCLUSION

The 3.5m mirror project is ambitious -- we face many difficult technical challenges -- but when we have successfully completed this project we will be prepared to work on the 8m mirrors that will follow.

### 9. ACKNOWLEDGEMENTS

I would like to thank the members of the Future Telescope Technology program whose accomplishments have been reported in this paper: Dave Dryden, John Fox, Charles Harmer, Bob Harris, Larry Junco, Bill Keppel (now on the staff of Embry-Riddle Aeronautical University), Lee Macomber, Liang Ming, Gary Poczulp, John Richardson, Mike Roman, Dan Towery, and Woon-Yin Wong. Significant contributions were also made by many other NOAO personnel, particularly Earl Pearson and Matt Johns. I am also grateful to Blain Olbert of Steward Observatory for measuring the stress levels in the mirror blank.

### 10. REFERENCES

1. M. Johns and C. Pilachowski, "The WIN 3.5 Meter Telescope Project", *Advanced Technology Optical Telescopes IV*, ed. L. D. Barr, vol. 1236, SPIE, Tucson, 1990.
2. "The NOAO 8-M Telescopes, II. Technical Description". Proposal to the National Science Foundation, p. D-7, 1989.
3. H. M. Martin, J. R. P. Angel and A. Y. S. Cheng, "Use of an actively stressed lap to polish a 1.8m f/1 paraboloid", *ESO Conference on Very Large Telescopes and Their Instrumentation*, ed. M.-H. Ulrich, Proc. No. 30, pp. 353-361, ESO, Garching, 1988.
4. C. Roddier and F. Roddier, "Interferogram analysis using Fourier transform techniques", *Appl. Opt.*, 26(9), pp. 1668-1673, 1987.
5. E. Pearson, "Hartmann test data reduction", *Advanced Technology Optical Telescopes IV*, ed. L. D. Barr, vol. 1236, SPIE, Tucson, 1990.
6. C. Roddier, F. Roddier, A. Stockton and A. Pickles, "Testing of telescope optics: a new approach", *Advanced Technology Optical Telescopes IV*, ed. L. D. Barr, vol. 1236, SPIE, Tucson, 1990.
7. E. Pearson, L. Stepp and W. Keppel, "Support of 8-meter borosilicate honeycomb mirrors", *ESO Conference on Very Large Telescopes and Their Instrumentation*, ed. M.-H. Ulrich, Proc. No. 30, pp. 435-449, ESO, Garching, 1988.

8. L. D. Barr, J. Fox, G. A. Poczulp and C. A. Roddier, "Seeing studies on a 1.8m mirror", *Advanced Technology Optical Telescopes IV*, ed. L. D. Barr, vol. 1236, SPIE, Tucson, 1990.
9. E. Pearson, L. Stepp, W-Y. Wong, J. Fox, D. Morse, J. Richardson and S. Eisenberg, "Planning the National New Technology Telescope (NNTT): III. primary optics - tests on a 1.8-m borosilicate glass honeycomb mirror", *Advanced Technology Optical Telescopes III*, ed. L. D. Barr, vol. 628, pp. 91-101, SPIE, Tucson, 1986.
10. W. Siegmund and L. Stepp, "Temperature control of large honeycomb mirrors", *Advanced Technology Optical Telescopes III*, ed. L. D. Barr, vol. 628, pp. 91-101, SPIE, Tucson, 1986.
11. A. Y. S. Cheng and J. R. P. Angel, "Steps toward 8m honeycomb mirrors VIII: design and demonstration of a system of thermal control", *Advanced Technology Optical Telescopes III*, ed. L. D. Barr, vol. 628, pp. 536-544, SPIE, Tucson, 1986.
12. M. Lloyd-Hart, "System for precise thermal control of borosilicate honeycomb mirrors during polishing and testing", *Advanced Technology Optical Telescopes IV*, ed. L. D. Barr, vol. 1236, SPIE, Tucson, 1990.
13. L. Barr, V. Coude Du Foresto, J. Fox, G. Poczulp, J. Richardson, C. Roddier and F. Roddier, "A large mirror testing facility at the National Optical Astronomy Observatories", submitted to *Opt. Eng.*
14. E. Pearson, L. Stepp and J. Fox, "Active Optics Correction of thermal distortion of a 1.8-meter mirror", *Opt. Eng.* 27(2), pp. 115-122, 1988.
15. D. Dryden and E. Pearson, "Multiplexed precision thermal measurement system for large structured mirrors", *Advanced Technology Optical Telescopes IV*, ed. L. D. Barr, vol. 1236, SPIE, Tucson, 1990.